International Journal of Mechanical, Industrial and Aerospace Sciences
ISSN: 2517-9950
Vol:9, No:3, 2015

Modelling of Organic Rankine Cycle for Waste Heat Recovery Process in Supercritical Condition

Jahedul Islam Chowdhury, Bao Kha Nguyen, David Thornhill, Roy Douglas, Stephen Glover

***Abstract*—**Organic Rankine Cycle (ORC) is the most commonly used method for recovering energy from small sources of heat. The investigation of the ORC in supercritical condition is a new research area as it has a potential to generate high power and thermal efficiency in a waste heat recovery system. This paper presents a steady state ORC model in supercritical condition and its simulations with a real engine's exhaust data. The key component of ORC, evaporator, is modelled using finite volume method, modelling of all other components of the waste heat recovery system such as pump, expander and condenser are also presented. The aim of this paper is to investigate the effects of mass flow rate and evaporator outlet temperature on the efficiency of the waste heat recovery process. Additionally, the necessity of maintaining an optimum evaporator outlet temperature is also investigated. Simulation results show that modification of mass flow rate is the key to changing the operating temperature at the evaporator outlet.

***Keywords*—**Organic Rankine cycle, supercritical condition, steady state model, waste heat recovery.

I. Introduction

A typical diesel engine, running at its best operating condition, can convert 45% of thermal energy into shaft energy; while gasoline engine converts a maximum of 35% [1]. Most of the energy produced by internal combustion engines is expelled to the environment. This expel of energy is one of the major causes of global warming and pollution. In order to reduce the emission and fuel consumption, recovering engine waste heat has been one of the focuses over the past decades. The waste heat recovery (WHR) system is used to collect heat from the exhaust or coolant and convert it into either mechanical or electrical power, which increases the thermal efficiency of the engine [2]. Several methods of waste heat recovery have proposed in the open literature such as Organic Rankine Cycle (ORC), Kalina Cycle, Trilateral Flash Cycle, Goswami Cycle [3]. Among these methods, the Organic Rankine Cycle (ORC) system is widely used for low grade heat recovery applications because of its simplicity and low maintenance requirement [3].

ORC consists of four major components: pump, evaporator, expander and condenser as shown in Fig. 1. Liquid refrigerant is pumped to the evaporator where it gets heated and vaporized by the engine exhaust. This vaporized fluid is then expanded and produced mechanical energy in the shaft of the expander. An additional device called generator is coupled with the expander shaft to convert mechanical energy into electrical power. Exhaust product from the expander is passed through the condenser where secondary cooling air removes extra heat from the liquid-vapor mixture and converts it into liquid form.

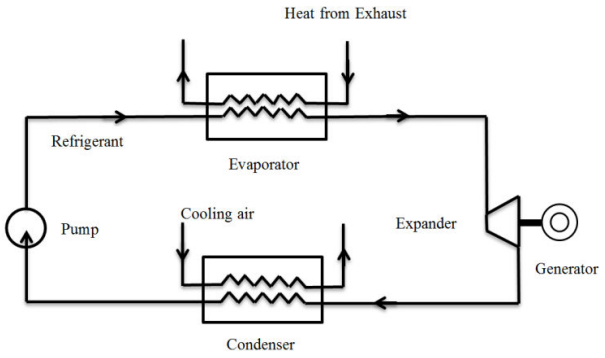

Fig. 1 A typical ORC

The working fluid used in the ORC is organic, which has the high molecular weight, high vapor pressure and low boiling point properties that are capable of producing more power from the low temperature heat sources [4]. Considering scale, efficiency, peak temperature and pressure of the waste heat recovery processes; ORC is the one proposed as best by many researchers [2], [5]-[7].

The ORC WHR can operate at two conditions: one is subcritical and the other is supercritical. Subcritical ORC uses a heat exchanger with the parameters below the critical pressure of the working fluid, whereas supercritical uses parameters above the critical pressure. The work output of an ORC in subcritical condition is low since the cycle is run by a lower pressure ratio. The heat addition of the working fluids in supercritical pressure can lead to the highest efficiency since specific work of the cycle is increased with the increase of pressure ratio [5]. In addition to the high work output of supercritical ORC, several benefits can be summarized as follows. Firstly, the critical pressure and temperature of organic fluids is much lower, and they can be elevated to a supercritical state without a high expense of compression work [3]. Secondly, the amount of exergy (available heat ready to work) destruction in the supercritical evaporator is much lower than that of a subcritical [8]. Another benefit is that the supercritical fluid does not go through a distinct liquid-vapor phase in the evaporator, thus a better thermal match between cold and hot fluid is achieved [9]. In general, a

J. I. Chowdhury, B. K. Nguyen, D. Thornhill, R. Douglas and S. Glover are with the School of Mechanical and Aerospace Engineering, Queen's University Belfast, Belfast, BT9 5AH, UK (corresponding author phone: +447468424610; e-mail: jchowdhury01@qub.ac.uk).

This work is a part of PhD project supported by the School of Mechanical and Aerospace Engineering, Queen's University Belfast, UK.

supercritical ORC can improve the thermal efficiency by 10% - 30% more than a subcritical ORC depending on the types of heat, fluids and cycle configuration used [3]. Moreover, the supercritical state of the organic fluids is easily achievable with the use of low grade energy [10]. Despite various benefits of the supercritical ORC, a high pressure in the system is led to concern about safety and availability of the components [11]. However, very few researches were found in literature on supercritical ORC, most of previous work has focused on the fluid selection [3], [12]; design and optimization [8], [10] only. In this work, a simulation of the ORC in supercritical condition with variable heat sources from the real vehicle exhaust is presented.

II. ORC Modelling

This section presents the modelling of all components in the ORC WHR system including: pump, evaporator, expander and condenser.

A. Pump

A volumetric diaphragm pump is selected for pumping the refrigerant to the evaporator. The relationship between mass flow rates and the pump speed in steady state is expressed as [13]:

$$\frac{\dot{m}_{p1}}{\dot{m}_{p2}} = \frac{N_{p1}}{N_{p2}} \tag{1}$$

where $\dot{m}_{p1}$ and $\dot{m}_{p2}$ are the mass flow rate of the pump in kg/s, and their corresponding pump speed (rpm) are N_{p1} and N_{p2} respectively. The relationship is derived from the performance curve of the selected pump [14] as follows.

$$\dot{m}_p = 0.00002 N_p + 0.0031 \tag{2}$$

For a given specific volume, $\bar{\upsilon}_p$ (m^3/kg) and mechanical efficiency of the pump, η_p outlet enthalpy and pump work are obtained, as [13].

$$H_{po} = \frac{\bar{\upsilon}_p (P_{po} - P_{pi})}{\eta_p} + H_{pi} \tag{3}$$

$$W_p = \frac{\bar{\upsilon}_p (P_{po} - P_{pi}) \dot{m}_p}{\eta_p} \tag{4}$$

where H_{pi} and H_{po} are the enthalpy of the fluid (KJ/kg) at inlet and outlet of the pump respectively, P_{pi} the pump inlet pressure, P_{po} the pump outlet pressure and W_p the pump work.

R134a is the working fluid used in the ORC circuit. The supercritical pressure at the pump outlet is set to 5500KPa which is above the critical pressure of R134a, 4060KPa. On the other hand, an inlet pressure of the pump, 1000KPa is used. Both pressures are assumed to be constant. It is also assumed that the mass flow rate of refrigerant for a single time step (0.25 s) is the same for all components.

B. Evaporator

Evaporator is the most critical part of the ORC. The thermal efficiency and heat recovery of the ORC is connected to the performance and parameters of the heat exchanger used in the system. In the proposed model, a counter current plate type heat exchanger operating under supercritical condition is the evaporator used in the ORC circuit. However, [8] shows that the thermo-physical properties of the fluids in supercritical condition are strongly dependent on temperature. Therefore, in order to capture those changes into account, splitting the evaporator along the flow direction is mandatory. For this reason, the evaporator is divided into 20 segments, as shown in Fig. 2, and heat transfer equation for each segment is solved by the finite volume method [15].

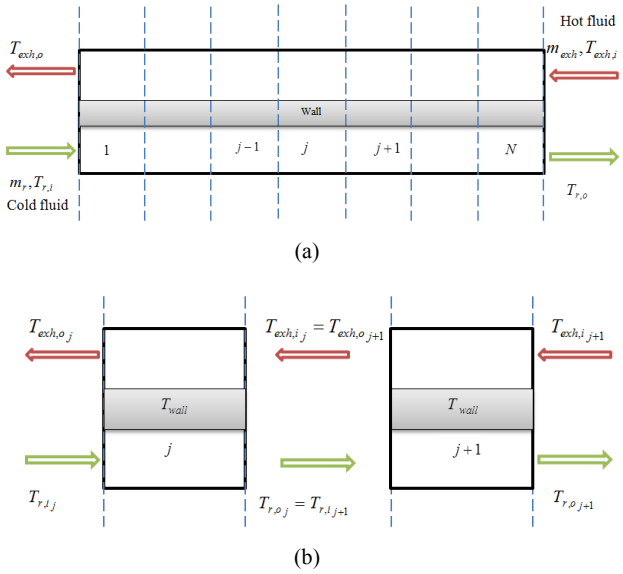

Fig. 2 (a) Finite volume evaporator model (b) Relationship between input-output of the adjacent segments

The model uses engine's exhaust as the hot fluid and refrigerant as the cold fluid as shown in Fig. 2. Corresponding inputs of the evaporator model are: mass flow rate and temperature of the exhaust and refrigerant. Since the outlet temperature of the hot and cold fluid is not known initially, an iteration process is carried out from the 1st segment to the N^{th} segment as shown in Fig. 2 (a). Fig. 2 (b) represents the relationship between input and output of the adjacent segments. For each cell, heat transfer from the exhaust to the wall and wall to the refrigerant are obtained with (5) and (6) respectively.

$$Q_{exh_j} = h_{exh_j} A_{exh_j} (T_{exh} - T_{wall})_j \tag{5}$$

$$Q_{r_j} = h_{r_j} A_{r_j} (T_{wall} - T_r)_j \tag{6}$$

where Q_{exh_j} and Q_{r_j} refer to the amount of heat (kW) that is transferred from the exhaust to the wall and wall to the refrigerant respectively. h_{exh_j} and h_{r_j} the convective heat transfer coefficients (kW/m^2 K) of exhaust and refrigerant with the wall. Both heat transfer coefficients are obtained correspond to the fluids average temperature in the cell or segment. A_{exh_j} and A_{r_j} are heat transfer surface area , T_{exh} and T_r are the exhaust and refrigerant's average temperature. T_{wall} the wall temperature which is the average of two fluids of the cell i.e.

$$T_{exh} = \frac{T_{exh,i} + T_{exh,o}}{2} \tag{7}$$

$$T_r = \frac{T_{r,i} + T_{r,o}}{2} \tag{8}$$

$$T_{wall} = \frac{T_{exh} + T_r}{2} \tag{9}$$

where $T_{exh,i}$, $T_{exh,o}$ are the exhaust temperature and $T_{r,i}$, $T_{r,o}$ the refrigerant temperature at the inlet and outlet of each segment.

TABLE I
ORC MODEL PARAMETER

Symbol	Quantity	Value
N	Number of segments of the evaporator	20
A	Heat transfer area of the evaporator	3m^2
$D_{h,g}$	Hydraulic diameter (gas side)	0.009m
$D_{h,l}$	Hydraulic diameter (liquid side)	0.004m
L	Length of each plate of the evaporator	0.3m
w	Width of each plate of the evaporator	0.119m
K	Thermal conductivity	15W/m K
$r_{v,i}$	Built in volume ration of the expander	6
η_{exp}	Expander mechanical efficiency	0.8
η_p	High pressure pump efficiency	0.75

Heat transfer due to change in temperature of the hot fluid can be calculated by (10) whereas heat transfer due to change in enthalpy of the refrigerant side is calculated by (11).

$$Q_{exh_j} = \dot{m}_{exh_j} C_{p,exh_j} (T_{exh,i} - T_{exh,o})_j \tag{10}$$

$$Q_{r_j} = \dot{m}_{r_j} (H_{r,o} - H_{r,i})_j \tag{11}$$

where $\dot{m}_{exh_j}$ (kg/s) and $\dot{m}_{r_j}$ (kg/s) are the mass flow rate of exhaust and refrigerant respectively, C_{p,exh_j} (KJ/kg K) the specific heat capacity of exhaust. H_{r_j} (KJ/kg) is the enthalpy of the refrigerant.

Nevertheless, the mass flow rate of refrigerant $\dot{m}_r$ is equal to the mass flow rate of the pump $\dot{m}_p$ used in the developed model. The convective heat transfer coefficients in (5) and (6) are calculated from the relationship among the Nusselt number, Nu Reynolds number, Re and Prandtl number, Pr as suggested in [16] and [8] respectively.

$$Nu = 0.2536 \mathrm{Re}^{0.65} \mathrm{Pr}^{0.4} \tag{12}$$

$$Nu = 0.023 \mathrm{Re}^{0.8} \mathrm{Pr}^{0.3} \tag{13}$$

$$Nu = \frac{hD_h}{K} \tag{14}$$

where D_h is the hydraulic diameter of the plate heat exchanger. The Reynolds number Re is calculated by

$$\mathrm{Re} = \frac{\rho V D_h}{\mu} \tag{15}$$

where ρ is the density (kg/m^3), μ the viscosity (Pa.s) and V the velocity of the fluids (m/s).

The supercritical pressure in the evaporator is assumed to be constant and thermal resistance of the wall is negligible. It is also assumed that the exhaust pressure is slightly higher than the atmospheric pressure and is constant throughout the evaporator. Exhaust power is obtained by

$$Q_{exh} = \dot{m}_{exh} (H_{exh,i} - H_{exh,ref}) \tag{16}$$

where $H_{exh,i}$ and $H_{exh,ref}$ are the enthalpy at the inlet temperature of exhaust and enthalpy at the reference temperature $25^o C$ of environment respectively.

C. Expander

Expander is a mechanical device which extracts heat energy and converts it into mechanical rotational energy. A scroll expander is chosen for the simulation purpose. The scroll expander has the low number of moving parts, reliability and leak proof quality that makes it an ideal candidate for the ORC application. The expansion work of a scroll expander is split into two parts [17]: One is isentropic expansion w_{isen} and other one is constant volume expansion w_{vol} .

$$w_{isen} = (H_{\exp,i} - H_{\exp,in}) \tag{17}$$

$$w_{vol} = r_{v,i} \upsilon_{\exp,i} (P_{\exp,in} - P_{con}) \tag{18}$$

where $H_{\exp,i}$ is the enthalpy at the expander inlet, $\upsilon_{\exp,i}$ the specific volume at inlet of the expander, $r_{v,i}$ the ratio of inlet to the outlet pocket volume of the expander, $P_{\exp,in}$ the expander internal pressure and P_{con} is the condenser pressure. This pressure is assumed to be equal to the pump inlet

pressure. Therefore, total work output $W_{\exp}$ and enthalpy at the outlet of expander $H_{\exp,out}$ are obtained by

$$W_{\exp} = \dot{m}_{\exp}\eta_{\exp}(w_{isen} + w_{vol}) \quad (19)$$

$$H_{\exp,out} = H_{\exp,i} - \frac{W_{\exp}}{\dot{m}_{\exp}} \quad (20)$$

where $\eta_{\exp}$ is the mechanical efficiency of the expander. All parameters used in the ORC model are listed in Table I.

D. Condenser

A thermodynamic model of the condenser based on the state enthalpy is represented by (21).

$$Q_{con} = \dot{m}_{con}(H_{\exp,out} - H_{p,i}) \quad (21)$$

where Q_{con} is the condenser cooling required (kW), $\dot{m}_{con}$ the mass flow rate of refrigerant through the condenser which is the same as the mass flow of refrigerant at the pump. $H_{p,i}$ the enthalpy at the inlet of the pump.

It is assumed that sufficient amount of cooling air is supplied to the condenser so that the liquid vapor refrigerant from the expander is cooled down to the initial pump inlet temperature. The consequences and output of the condenser model are not included in the results and discussion part as this component has been used for completing the ORC cycle only.

E. Performance Evaluation

The performance of the ORC is described by three basic parameters. These are: cycle efficiency, heat recovery efficiency and overall system efficiency [5].

$$\eta_{cy} = \frac{W_{Net}}{Q_{ev}} \quad (22)$$

$$\eta_{HR} = \frac{Q_{ev}}{Q_{exh}} \quad (23)$$

$$\eta_{oall} = \eta_{cy} \times \eta_{HR} \quad (24)$$

where η_{cy} is the cycle, η_{HR} the heat recovery, η_{oall} overall system efficiency. Q_{ev} the evaporator power which is obtained by (11), Q_{exh} the exhaust heat power calculated in (16).The net work output W_{net} in (22) is calculated by

$$W_{net} = (W_{\exp} - W_p) \quad (25)$$

III. Simulation

The supercritical ORC model for WHR process presented in this paper is built in Matlab environment and simulated with the exhaust data of a highway drive cycle from a hybrid - General Motors (GM) car. The selected exhaust data in terms of mass flow and temperature profile are shown in Figs. 3 and 4. For simplicity of calculation, it is assumed that the properties of air are exactly same to the properties of exhaust gas. On the other hand, developed mode uses R134a refrigerant as the working fluid that is circulated through the ORC circuit. All thermo-physical properties of air and R134a are obtained from the NIST (National Institute of Standard and technology) database called REFPROP [18].

Simulation of the waste heat recovery process is presented with entire operating points and with a selected point of vehicle drive cycle data. A random pump speed regulates the mass flow of refrigerant is used as the input to the pump for the simulation of entire operating period of time. In order to keep the output evaporator temperature within the allowable range as set by REFPROP, the input pump speed ranges are set from 1000 rpm to 1750 rpm. But the ranges of the pump speed used for specific operating point simulation is set to 400-1750rpm since the heat source mass flow and temperature is lower for this case and is not able to produce very high evaporator temperature beyond the acceptable range. Figs. 5-10 show the results of the entire operating points while Figs. 11-13 show the results of the specific operating point.

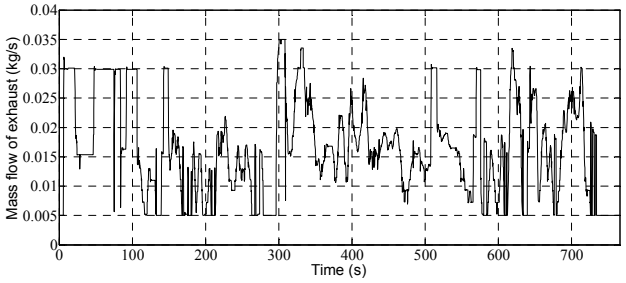

Fig. 3 Mass flow rate of exhaust for GM highway drive cycle

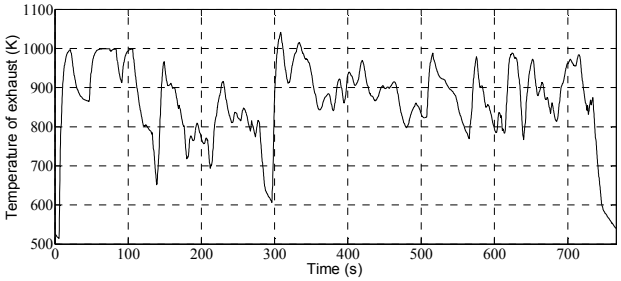

Fig. 4 Temperature of exhaust for GM highway drive cycle

Fig. 5 shows the variation of heat power absorbed by the evaporator for a given exhaust profile. A maximum of 16.5 kW heat is recovered from the exhaust flowing at 0.035kg/s and at a temperature of 1041K. The variation of evaporator temperature is presented in Fig. 6, in which a maximum temperature of 650K is noticed. However, there are two limiting factors which need to be considered when simulating R134a in supercritical condition: one is the upper limit of the evaporator temperature which is bounded by its auto ignition temperature of 773K; other one is the REFPROP which is

limited to provide properties up to the temperature of 682K.

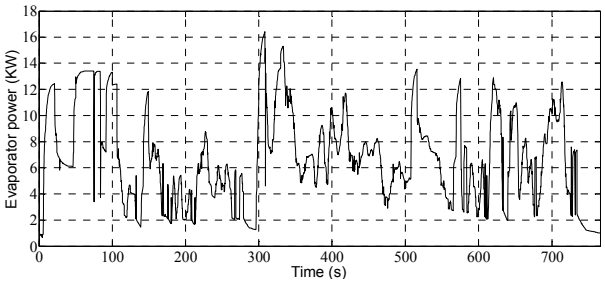

Fig. 5 Evaporator power recovered over entire operating period

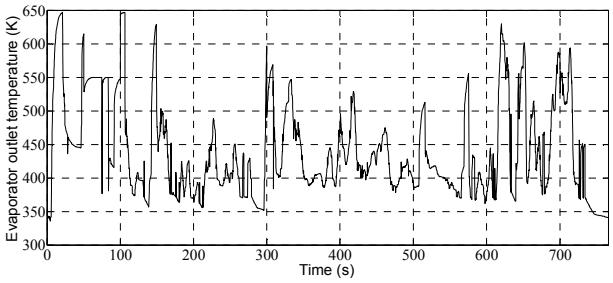

Fig. 6 Evaporator outlet temperature over entire operating period

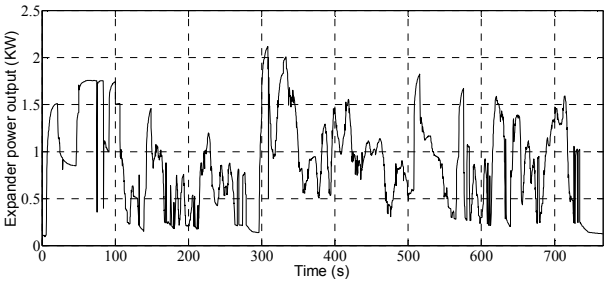

Fig. 7 Expander power output over entire operating period

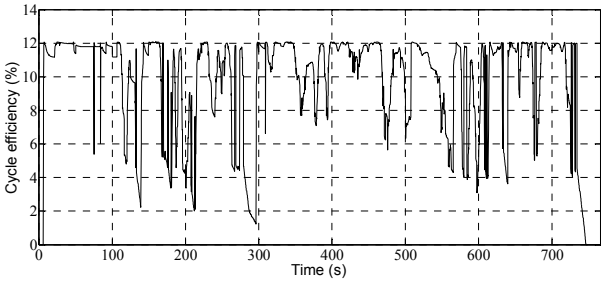

Fig. 8 Cycle efficiency over entire operating period

A vehicle drive cycle is generally capable of producing 1-2kW of power at the expansion device. However, the supercritical ORC model produces a maximum of 2.1kW power as shown in Fig. 7.

The cycle efficiency of the model for variable heat sources is presented in Fig. 8. It can be seen that cycle efficiency fluctuates from around 2% to around 12.05% depending on the combination of mass flow and temperature of the exhaust and refrigerant. It can also be noticed that the cycle efficiency at some points become zero. This may arise when the power required at the pump is equal to or higher than the power output of an expander. On the other hand, the developed ORC model is able to recover as minimum as 55% to slightly over 80% of heat from the specified exhaust flow as shown in Fig. 9. An overall system efficiency calculated with (24) is shown in Fig. 10. A maximum of 8.05% overall efficiency is noticed.

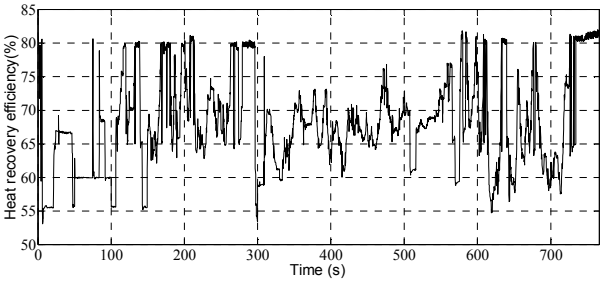

Fig. 9 Heat recovery efficiency over entire operating period

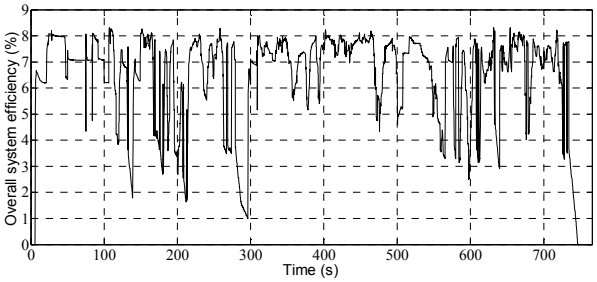

Fig. 10 Overall system efficiency over entire operating period

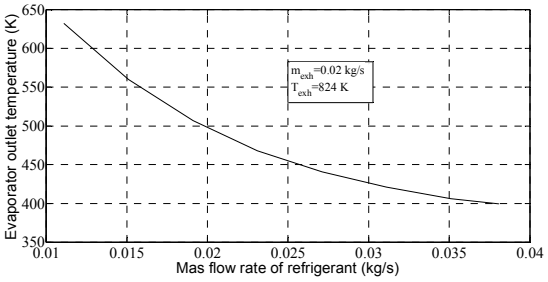

Fig. 11 Relationship between mass flow of refrigerant and evaporator outlet temperature

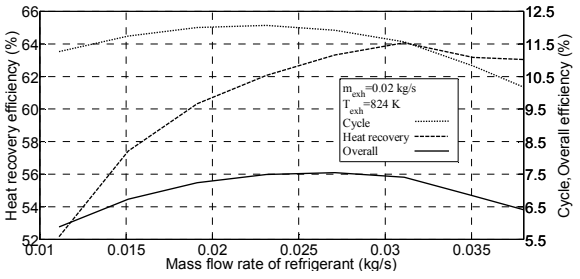

Fig. 12 Effect of mass flow rate of refrigerant on efficiency

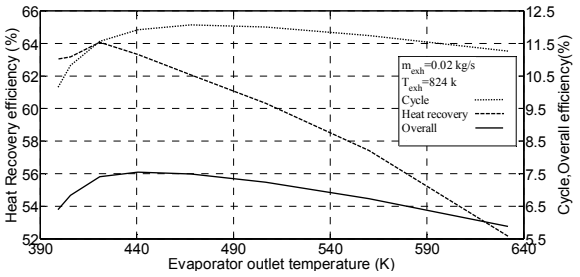

Fig. 13 Effect of evaporator outlet temperature on efficiency

The relationship between mass flow rate of refrigerant and evaporator outlet temperature for specific operating point is shown in Fig. 11. For a given exhaust flow and temperature, the evaporator outlet temperature decreases exponentially with the increase of the refrigerant flow. The relationship between refrigerant flow and the efficiency is shown in Fig. 12. It can be seen, as the mass flow rate increases, the cycle efficiency also increases up to a point where it reaches maximum, after that it declines. On the contrary, an improvement of the heat recovery efficiency is possible with the higher rate of refrigerant. An optimum point between two performance indicators can be derived with the third indicator called overall system efficiency.

A similar analysis for evaporator temperature is shown in Fig. 13. Results show that an increasing in the evaporator temperature causes a decrease in the heat recovery efficiency because the expander exhaust is cooled down at the higher temperature. Nevertheless, an optimum temperature of 470K is the one which gives the highest efficiency of the ORC. Fig. 13 shows the highest cycle efficiency of 12.05% and a corresponding heat recovery efficiency of 64% is observed at the optimum temperature of 470K. Therefore, combining Figs. 11-13, a conclusion can be drawn that the highest efficiency of the ORC can be obtained with the optimum temperature but not with the higher or lower temperature.

IV. Conclusion

The steady state ORC model simulated with the variable exhaust data from a vehicle drive cycle is presented in this paper. Conclusions from the simulation outcomes can be drawn as follows:

1) A steady state model is suitable to visualize the effect of the mass flow rate of the refrigerant on the evaporator outlet temperature which is the critical parameter needs to be controlled in real time.
2) A steady state model with the entire operating points can provide an overall mapping and characterization of operating ranges of the waste heat recovery process.
3) A higher temperature at the evaporator outlet is not able to provide highest cycle efficiency; but an optimum temperature of the system can effectively utilize the heat and deliver maximum efficiency.
4) A fast response of the evaporator parameters is reported in the steady state model since the model is not taken thermal inertia into account. Further development of this model could be achieved by modelling of thermal inertia within the waste heat recovery process.

References

[1] A. Boretti, "Recovery of exhaust and coolant heat with R245fa organic Rankine cycles in a hybrid passenger car with a naturally aspirated gasoline engine," *Applied Thermal Engineering,* vol. 36, pp. 73-77, April 2012.

[2] S. Glover, R. Douglas, L. Glover and G. McCullough, "Preliminary analysis of organic Rankine cycles to improve vehicle efficiency," *Proceedings of the Institution of Mechanical Engineers, Part D: Journal of Automobile Engineering,* vol. 228, no. 10, pp. 1142-1153, April 2014.

[3] H. Gao, C. Liu, C. He, X. Xu, S. Wu and Y. Li, "Performance Analysis and Working Fluid Selection of a Supercritical Organic Rankine Cycle for Low Grade Waste Heat Recovery," *Energies 2012,* vol. 5, pp. 3233-3247, Aug. 2012.

[4] J. Zhang, Y. Zhou, Y. Li, G. Hou and F. Fang, "Generalized predictive control applied in waste heat recovery power plants," *Applied Energy,* vol. 102, pp. 320–326, Feb. 2013.

[5] S. Quoilin, R. Aumann, A. Grill, A. Schuster, V. Lemort and H. Spliethoff, "Dynamic modeling and optimal control strategy of waste heat recovery Organic Rankine Cycles," *Applied Energy,* vol. 88, pp. 2183-2190, June 2011.

[6] D. Ziviani, A. Beyene and M. Venturini, "Advances and challenges in ORC systems modeling for low grade thermal energy recovery," *Applied Energy,* vol. 121, pp. 79–95, May 2014.

[7] H. G. Zhang, E. H. Wang and B. Fan, "Heat transfer analysis of a finned-tube evaporator for engine exhaust heat recovery," *Energy Conversion and Management,* vol. 65, pp. 438–447, Jan. 2013.

[8] S. Karellasa, A. Schusterb and A.-D. Leontaritis, "Influence of supercritical ORC parameters on plate heat exchanger design," *Applied Thermal Engineering ,* vol. 33, no. 34, pp. 70-76, Feb. 2012

[9] B. Saleh, G. Koglbauer, M. Wendland and J. Fischer, "Working fluids for low-temperature organic Rankine cycles," *Energy,* vol. 32, pp. 1210–1221, July 2007.

[10] A. Schuster, S. Karellas and R. Aumann, "Efficiency optimization potential in supercritical Organic Rankine Cycles," *Energy,* vol. 35, pp. 1033–1039, Feb. 2010.

[11] H. Chen, D. Y. Goswami and E. K. Stefanakos, "A review of thermodynamic cycles and working fluids for the conversion of low-grade heat," *Renewable and Sustainable Energy Reviews,* vol. 14, pp. 3059–3067, Dec. 2010.

[12] S. Glover, R. Douglas, L. Glover, G. McCullough and S. McKenna, "Automotive Waste Heat Recovery: Working Fluid Selection and Related Boundary Conditions," *International Journal of Automotive Technology,* submitted for publication.

[13] J. Zhang, Y. Zhou, R. Wang, J. Xu and F. Fang, "Modeling and constrained multivariable predictive control for ORC (Organic Rankine Cycle) based waste heat energy conversion systems," *Energy,* vol. 66, pp. 128-138, March 2014.

[14] Wanner Engineering, Inc., *Hydra-Cell industrial pumps -installation and service D03-991-2400A,* Minneapolis, USA.

[15] J. Patiño, R. Llopis, D. Sánchez, C. Sanz-Kock, R. Cabello and E. Torrella, "A comparative analysis of a CO2 evaporator model using experimental heat transfer correlations and a flow pattern map," *International Journal of Heat and Mass Transfer,* vol. 71, pp. 361–375, April 2014.

[16] R. Buonopane, R. Trupe and J. Morgan, "Heat transfer design method for plate heat exchangers," *Chemical Engineering Progress,* vol. 59, no. 7, pp. 57-61, 1963.

[17] S. Quoilin, V. Lemort and J. Lebrun, "Experimental study and modeling of an Organic Rankine Cycle using scroll expander," *Applied Energy,* vol. 87, pp. 1260-1268, April 2010.

[18] "www.NIST.gov," *NIST Reference Fluid Thermodynamic and Transport Properties Database (REFPROP): Version 9*, 2010. (Online). (Accessed November 2010).